UNIVERSITY OF LEEDS

This is a repository copy of *Understanding Catalyst Overheating Protection (COP) as a Source of Post-TWC Ammonia Emissions from Petrol Vehicle*.

White Rose Research Online URL for this paper:
https://eprints.whiterose.ac.uk/191338/

Version: Accepted Version

White Rose
university consortium
Universities of Leeds, Sheffield & York

eprints@whiterose.ac.uk
https://eprints.whiterose.ac.uk/

Understanding catalyst overheating protection (COP) as a source of post-TWC ammonia emissions from petrol vehicle

Author, co-author (Do NOT enter this information. It will be pulled from participant tab in MyTechZone)

Affiliation (Do NOT enter this information. It will be pulled from participant tab in MyTechZone)

Abstract

TWC exposure to extreme temperature could result in irreversible damage or thermal failure. Thus, a strategy embedded in the engine control unit (ECU) called catalyst overheating protection (COP) will be activated to prevent TWC overheating. When COP is activated, the command air-fuel ratio will be enriched to cool the catalyst monolith down.

Fuel enrichment has been proven a main prerequisite for ammonia formation in hot TWCs as a by-product of NOx reduction. Hence, COP events could theoretically be a source of post-catalyst ammonia from petrol vehicles, but this theory is yet to be confirmed in published literature. This paper validated this hypothesis using a self-programmed chassis-level test. The speed of the test vehicle was set to constant while the TWC temperature was raised stepwise until a COP event was activated. It is observed that at both testing speeds, the ammonia spike identified by a Fourier-transformation infrared analyzer (FTIR) spectrometer accorded well with the COP fuel enrichment command obtained with an OBD scan tool and downstream CO/THC concentrations once the TWC temperature exceeded a certain threshold. This confirms that COP events could result in excessive ammonia emission from petrol vehicles. In addition, a non-negligible impact of the presence of condensed water in the sample line on the quantification of ammonia (particularly on the decay side) was noticed, which could challenge the forthcoming legislation.
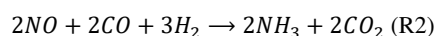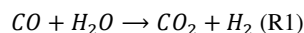
Introduction

As a key secondary aerosol neutralizer, ammonia emissions from vehicles have been shown to have significantly contributed to the hazy weather occurring in Chinese metropolitan areas [1]. Although in a 2011 EEA report, the transport sector has been ranked as a source giving greater anthropogenic ammonia compared to the industrial processes and waste decomposition [2]. Still, the importance of transport-related ammonia emissions might have been underestimated, particularly its contribution to the formation of secondary particles [3,4]. A more recent study revealed that the cost effectiveness of the control anthropogenic ammonia emissions has surpassed nitrogen oxides (NO_x) in abating secondary particulate matter [5].

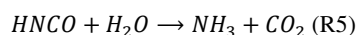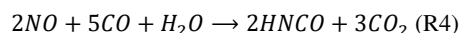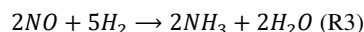Both diesel and gasoline vehicles emit ammonia. Ammonia emissions from diesel vehicles are in general slips from the selective catalytic reduction (SCR) systems, which have been regulated in the heavy-duty emission regulations worldwide. In contrast, ammonia from petrol vehicles is globally non-regulated, though the awareness of its existence can date back to the 1960s [6]. In the early 1980s, Smith and Black observed the formation and release of ammonia on TWC [7]. Based on annual remote sensing data, Carslaw and Phys-Tyler pointed out that transport-related ammonia has consistently contributed to the increased urban ammonia level in British cities since the popularization of TWC after model year 1992 [8].

Ammonia from petrol vehicles is a TWC by-product when reducing nitrogen oxides to nitrogen [9-12]. Several studies have investigated the mechanisms of post-catalyst ammonia formation, either at engine level or using bench reactors. It is widely acknowledged that ammonia is formed on hot TWCs and favored by enriched air-fuel mixtures [10,13]. Reactions (R1) to (R11) summarize the possible reaction routes for ammonia formation on a hot TWC [14-17].

Fundamental pathways:

$$CO + H_2O \longrightarrow CO_2 + H_2 \text{ (R1)}$$

$$2NO + 2CO + 3H_2 \longrightarrow 2NH_3 + 2CO_2 \text{ (R2)}$$

Pathways via HNCO:

$$2NO + 5H_2 \longrightarrow 2NH_3 + 2H_2O \text{ (R3)}$$

$$2NO + 5CO + H_2O \longrightarrow 2HNCO + 3CO_2 \text{ (R4)}$$

$$HNCO + H_2O \longrightarrow NH_3 + CO_2 \text{ (R5)}$$

Hydrogen generated via hydrocarbons, hydroxyl and other pathways:

$$C_3H_8 + 3H_2O \longrightarrow 7H_2 + CO \text{ (R6)}$$

$$CH_4 + H_2O \longrightarrow 3H_2 + CO \text{ (R7)}$$

$$2OH + 2CO \longrightarrow 2CO_2 + H_2 \text{ (R8)}$$

$$2NO_x + (2x + 3)H_2 \longrightarrow (2x + 3)H_2O + 2NH_3 \text{ (R9)}$$

$$2NO + 2H_2 \longrightarrow N_2 + 2H_2O \text{ (R10)}$$

04/19/2022

$6NO + 4NH_3 \rightarrow 5N_2 + 6H_2O$ (R11)
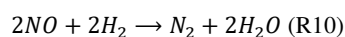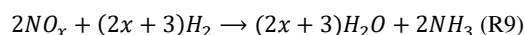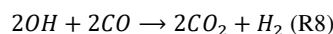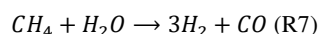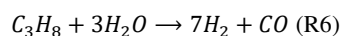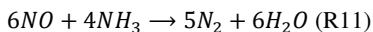
In general, ammonia formation on a hot TWC surface can be divided into two main steps:

- STEP 1: Incomplete oxidation resultants, CO and hydrocarbons, form hydrogen via water-gas or steam-reforming reactions with Pt/Pd being the catalysts;
- STEP 2: Hydrogen reacts with NOx with the aid of Rh-catalyst or via dihydroxylation reactions on the surface of CeO_2, and release ammonia [16].

This process helps explain the observed high ammonia emissions corresponding to engine warm-up duration reported by Wang et al. [4], and the release of excessive ammonia emissions under aggressive driving style and high engine load conditions observed by Huai and Heeb et al., which may mandate enriched air-fuel mixtures for better dynamic performance [13,18]. Similarly, using vehicle specific power (VSP) as an indicator, Huang and Han et al. pointed out that ammonia emission positively correlated to VSP when the test vehicles were at constant speeds or in accelerations [19,20]. Besides, Sun et al. also noticed excessive ammonia emissions in real-world emission measurement as road slope and the frequency of engine stop-and-go increased [21].

Considering that petrol ammonia emission is predominantly by hot TWC and enriched mixture, it is reasonable to hypothesize that a catalyst overheating protection event, which happens when the catalyst is hot and requires fuel enrichment, could also be a source of post-catalyst ammonia emission in addition to the regular fuel-rich conditions mentioned above.

COP is a strategy to prevent TWCs from overheating and to avert the related damages, such as melting or cracking. Catalyst overheating is a phenomenon that could sometimes happen during routine driving, especially for small engines. Along with the global application of ever tightening fuel economy regulations and therefore engine down-sizing, the frequency of COP calling has been shown to be climbing [22].

Multiple reasons could result in catalyst overheating, the most straight-forward one is long-time operation at high engine loads, which may come along with motorway and aggressive driving behaviors. Heat accumulates inside the monolith and the TWC temperature keeps climbing. For vehicles with heavier payloads but smaller engines, light commercial vehicles for instance, such a phenomenon could be sometimes seen during the WLTC tests.

Besides, catalyst overheating can also be a consequence of over-retarded ignition timing to prevent engine knock. When ignition timing is retarded, the temperature of the exhaust and catalyst monolith increases because more of the combustion heat is rejected to the exhaust system instead of being contained in the combustion chamber and absorbed by the coolant. For down-sized engines, the negative effects of retarding ignition timing could be more pronounced because of reduced areas for heat transfer [22].

Some other factors could induce catalyst overheating as well. For vehicles with manual gearboxes for example, if no special attentions were paid during the R&D process, catalyst overheating could happen within the gear selecting operations due to an engine down-to-idle (DTI) event. During this event, a rapid and remarkable drop in the exhaust flow rate causes heat accumulation in the monolith.

04/19/2022

Driven by the implementation of Real Driving Emission (RDE) regulation in the EU and China, an increasing number of new models decided to employ gasoline particulate filters (GPFs). For GPF-equipped vehicles, if the regeneration event occurs unexpectedly late, (e.g. long-time creeping induced no high enough exhaust temperature to initiate a regeneration) then the oxidation of over-loaded soot could markedly increase the risk of catalyst overheating.

No matter which mechanism underlines catalyst overheating, when the engine control unit detects and believes that overheating could occur, it is tuned to enrich the air-fuel mixture for protection purposes since compared to the stoichiometric mixture, slightly enriched mixtures decrease the exhaust temperature and knock tendency [22,23]. However, this possibly favors the formation of post-catalyst ammonia.

Previous studies mainly focused on the reaction pathways governing ammonia formation and the determination of ammonia emission factors over various drive cycles. Compared to the tens of milligrams per kilometer travelled of earlier models [10,13,18,24-27], ammonia emissions from the majority of tested Euro-5 and Euro-6 vehicles have been reduced to a level around 10 mg/km. Bielaczyc and Woodburn et al. compared the ammonia emissions from vehicles fueled with petrol, LPG, and CNG over the New European Drive Cycle (NEDC) [11,28,29]. Petrol and LPG resulted in an equal ammonia emission factor of 6.7 mg/km, while ammonia emissions with CNG fueling ranged from 2.34-11.3 mg/km, which showed no clear tendency compared to petrol. Suarez-Bertoa et al. compared the ammonia emissions from modern petrol, diesel, and hybrid vehicles over the NEDC and WLTC [15,30-32]. In both room-temperature and low-temperature tests, the diesel test vehicles emitted less ammonia than the petrol. The hybrid test vehicle showed better ammonia emission control than the engine-only models. Both low-temperature operation and E85 fueling increased the ammonia emissions, with the impact of using E10 unclear in the test fleet.

Although a marginal decrease in ammonia emissions has been realized together with the more precise control of modern TWC technologies, the necessity to better understand and control possible ammonia sources in routine driving remains. This is due to the possibility of petrol ammonia becoming a criteria pollutant in the forthcoming regulations increases. Besides, on-road measurements of petrol ammonia emission also highlighted its severity and contribution to urban $PM_{2.5}$ contamination [33,34].

Based on the formation mechanisms of post-catalyst ammonia, a COP event, which may happen sometimes in real driving but be seldomly encountered in laboratory tests, is in theory a source of excessive ammonia emission from petrol vehicles. However, to the best knowledge of the authors, the correlation between COP fuel enrichment and ammonia emission has not been investigated before. In this paper, using a self-programmed drive cycle, which successfully commanded COP fuel enrichment at two constant vehicle speeds, the influences of COP activation on ammonia formation from a China-6 compliant compact SUV were examined and confirmed at chassis level with an FTIR spectroscope.

Materials and methodology

Test equipment

The test work of this paper was done in an emission certification laboratory based in Beijing, China. Figure 1 depicts a rig of the chassis-level ammonia emission measurement system.
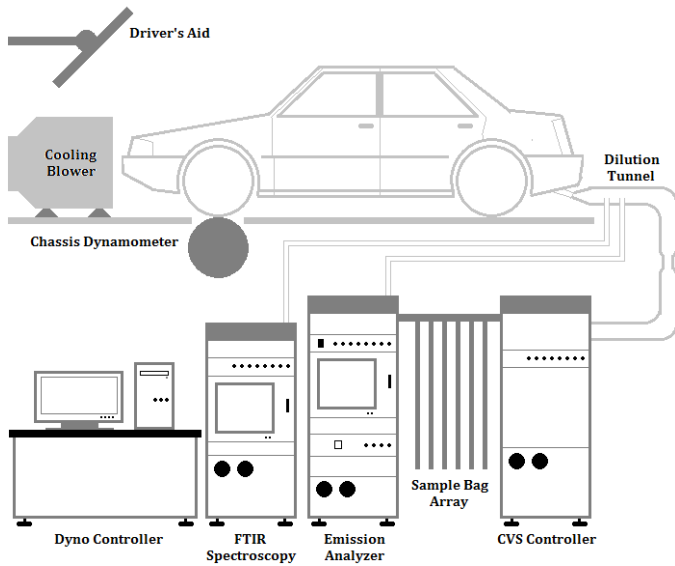
Figure 1. Chassis-level ammonia measurement system

As illustrated, to capture the ammonia releasing phenomenon corresponding to COP strategy activation, the test vehicle was placed in a temperature- and humidity-adjustable climate chamber (IMTECH SFTP, Germany) and fastened on a 48-inch roller chassis dynamometer (MAHA ECDM-48L-4WD, Germany). Post-catalyst ammonia, together with other reactive nitrogen compounds (NO, NO_2 and N_2O) related to ammonia formation and consumption, were measured using an FTIR spectroscopy analyzer (HORIBA MEXA-6000FT, Japan), while the regulated pollutants, including CO, CO_2, NO_x, and total hydrocarbons (THC), were measured with a multi-component emission analyzer (HORIBA MEXA-7400LE, Japan). In this research, ammonia and other reactive nitrogen compounds were measured undilutedly, while the regulated pollutants were quantified using a constant volume sampling system (HORIBA CVS-7400S, Japan). The sampling probes of the FTIR spectroscope were inserted into the conjunction between tailpipe exit and the exhaust entrance of the CVS. To minimize the artifact induced by exhaust-containing water vapor condensation and its adsorption of ammonia, both the sampling probe and lines were heated to 191°C. A dilution air purification system (HORIBA DAR-3300, Japan) was also employed to reduce the uncertainty associated with contaminated dilution air. Table.1 details the technical specifications of the experimental system.

Table 1. Specifications of the ammonia measurement system

Instrument model	Specifications	Accuracy
Climate chamber, IMTECH SFTP	Temperature: -35-60°C	Temperature: ±1°C in time & unevenness w/o heat load
Chassis-dyno, MAHA ECDM-48L-4WD	Max. 150kW, 200km/h, 4t inertia	Speed detector: 0.01km/h

Emission analyzer, HORIBA MEXA-7400LE	CO(l): NDIR, 0-3000ppm CO(h): NDIR, 0-10% CO_2: NDIR, 0-16%	1ppm or 0.2% of FS, whichever is smaller
FTIR spectroscopy, HORIBA MEXA-6000FT	Sample line heated to 191°C, response time shorter than 5s	Repeatability: within 1% of FS Zero drift/noise: <1% of FS
Dilution air purifier, HORIBA DAR-3300	Max. 3300m³/min	CO, HC, and NO_x: 0.1ppm or less

In addition to the emission concentrations, some key engine operating parameters, including vehicle speed, engine load, catalyst temperature, and lambda (excess air ratio) command, were collected from the OBD port using a SAE J1978 compliant CAN hardware (Kvaser USBcan Pro, Sweden) with a GUI software (RA Silverscan, Germany). During the test, the OBD readings of vehicle speed and engine load were also used together with a driver's aid to allow the driver to maintain constant-speed driving.

The sampling frequency of the emission analyzer, FTIR spectroscope, and OBD scan tool was set to 1Hz to simplify the time-alignment of data post-processing. Before the start of testing, the emission analyzer was calibrated with zero and span gases with known species and concentrations. Given the inability of an FTIR calibration, a functionality check of the ammonia measurement was done by releasing pure nitrogen and 500ppm ammonia span gas near the sampling probe before the measurement.

Test vehicle and fuel

The test vehicle of this research was a China-6a compliant (CO, THC, and NO_x limits are 700, 50, and 60mg/km over the WLTC at room temperature) compact sport utility vehicle (SUV), which had run roughly 13000km (laboratory-aged only) when tested. The specifications of the test vehicle are listed in Table.2.

Table 2. Specifications of the test vehicle

Item	Value
Model type	In-line, 4-cylinder, naturally-aspirated, DOHC, water-cooling
Displacement	1499mL
Bore	75mm
Stroke	84.8mm
Rated power	78kW @ 6000rpm
Maximum torque	145Nm @ 4300-4500rpm
Transmission	5-speed manual
Curb weight	1378kg
Tire	215/55 R18
Emission category	China-6a (model year 2017)

RON92 China-VIA gasoline purchased from a qualified refinery was fed to this test vehicle throughout the test. The standard mandates that China-VIA gasoline shall contain sulfur≤10ppm, benzene≤0.8vol%, aromatics≤35vol%, olefins≤18vol% and prohibits the use of Mn- or Fe-containing additives. Before the testing, the tire pressure of the test vehicle was adjusted to the manufacture default.
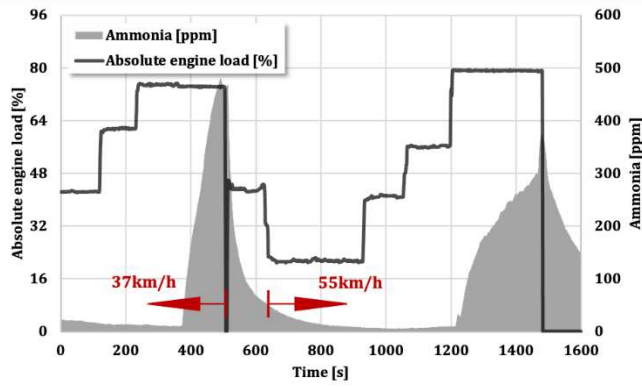
Test conditions

Figure 2. Vehicle speeds and engine loads have been examined in this research

The test vehicle was driven in accordance to a self-programmed driving cycle, in which the COP strategy was successively activated twice under two constant-speed conditions, namely 37km/h and 55km/h. This is shown in Figure 2. Testing was performed using the constant-speed mode of chassis-dyno. In this mode, the chassis-dyno worked in a way very similar to engine-dynos: the vehicle speed (and engine speed since all the measurements at 37km/h and 55km/h were made at fixed 3rd and 4th gear respectively to guarantee that the engine speed was relatively low) was maintained at a constant by the roller of the dyno, so pressing the accelerator deeper only increased the throttle openness and engine load and therefore the temperature of exhaust. Table 3 lists the operating conditions that have been tested in this research.

Within this ~1600s cycle driving, two COP events were activated at roughly 80% of engine load. Due to no access to change the engine control parameters, in this research, COP events were only managed to be activated by forcing the engine to run continuously at relatively low speeds but high loads, which created an unfavorable condition for catalyst cooling. This driving pattern mimicked longtime uphill driving in actual scenario.

Table 3. Test conditions of this research

Vehicle speed	Absolute engine load read from OBD (duration)
37km/h	42.0% (0-120s), 61.0% (120-230s), 75.0% (230-500s)
55km/h	22.0% (640-930s), 41.0% (930-1050s), 56.0% (1050-1200s), 80.0% (1200-1480s)

Data uncertainty

Since the engine load of the test vehicle was increased stepwise at each testing speed, the measurement of all exhaust emissions during each operating condition was a quasi-steady-state process, which was held for at least 110s. This feature allowed each measurement to have sufficient repeatability and credibility. The uncertainty of the results of this research primarily came from: 1) the inaccuracy of ammonia quantification using an FTIR spectroscope, and 2) ammonia absorbed by condensed water in the engine exhaust. The latter could play a more dominant role in the uncertainty because according to the readings of the FTIR, the measured water vapor was always smaller than the theoretical value of stoichiometric petrol combustion, suggesting the existence of liquid water in the tailpipe which would reduce the peak value of ammonia.

But, given that the aim of this research is to qualitatively validate the linkage between a COP event and the formation of post-catalyst ammonia from petrol vehicles, these two sources of uncertainty will not result in a biased conclusion.

Results and discussion
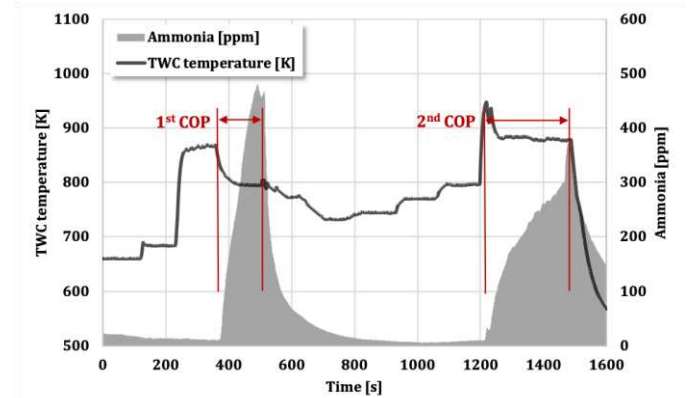
COP-induced ammonia emission

Figure 3. Ammonia versus TWC temperature with the presence of COP

Figure 3 illustrates the second-by-second record of the TWC temperature using the OBD scan tool together with the ammonia concentrations as a function of time. It must be declared that the TWC temperature provided in Figure 3 was predicted temperature using calibration data and the model embedded in the ECU, empirically a manufacturer-dependent difference of at most 50°C may exist compared with sensor measurement. The two artificially activated COP windows are marked with red arrows.

It can be seen in Figure 3 that at each vehicle speed, the TWC temperature also increased stepwise with engine load, but when the engine load was raised to about 80%, TWC temperatures grew sharply until the activation of a COP strategy in both cases. This is because at fixed engine speed (due to fixed vehicle speed and gear), both the fuel injection and in-cylinder combustion durations became longer at higher loads. A larger amount of heat tended to be released towards the end of expansion stroke, close to the exhaust valve opening, resulting in increased exhaust temperature.
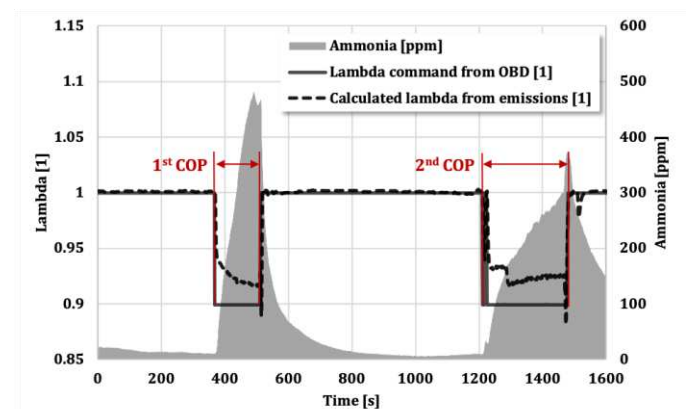

Figure 4. Ammonia versus lambda command and actual lambda with the presence of COP

At 37km/h, the TWC temperature jumped to about 570°C after the engine load was raised to 75%. The temperature of the TWC then continued rising at a slower pace when the engine load stabilized around 75% for roughly 130s, until the first COP enrichment was triggered at 580°C. It can be seen in Figure 4 that once a COP event occurred, enriched air-fuel mixture with a lambda of 0.9 was immediately commanded to cool down the TWC monolith. This is because the combustion and propagation rate of fuel-rich mixtures are faster than those of stoichiometric mixtures, letting more heat be absorbed by the engine coolant, and therefore alleviating the thermal burden of the exhaust system. As depicted in Figure 3, in the first 20s after the first activation of a COP strategy, the ECU-predicted TWC temperature dropped by approximately 70°C. Although the temperature of the TWC had been reduced to below 430°C (and COP "threshold" temperature) after the intervention of fuel enrichment, the COP strategy lasted for about 130s and then quitted until the TWC temperature stabilized. In Figure 4, the formation and release of ammonia well-aligned with COP-induced fuel enrichment, confirming catalyst overheating protection as a possible ammonia source for real driving petrol vehicles, which could be seldomly encountered in laboratory tests.

It should be explained that two lambda values are plotted in Figure 4, lambda command read from the OBD port, and actual lambda calculated based on the exhaust emission concentrations and fuel combustion chemistry. The calculation of actual lambda was on a basis of oxygen balance, which can be written as Eq.1 to Eq.4 [23].

$$\left(\frac{A}{F}\right) = 4.773 \left(\frac{M_{air}}{M_{fuel}}\right) \frac{[CO_2] + 0.5[CO] + 0.5[H_2O] + [O_2]}{[THC] + [CO] + [CO_2]}$$

(Eq.1)

$$[H_2O] = 0.5y \frac{[CO_2] + [CO]}{1 + [CO]/3.5[CO_2]}$$

(Eq.2)

$$M_{air} = 28.96, M_{fuel} = 12.01 + 1.008y, y = 1.87$$

(Eq.3)

$$\lambda = (A/F)/14.6$$

(Eq.4)

Where, *(A/F)* represents the air-to-fuel ratio, *[pollutant]* indicates the concentration in the unit of part per million (ppm) of an exhaust pollutant, *M_{air}* and *M_{fuel}* are the molecular weights of air and fuel, the values of which are given in Eq.3.

The purpose of using both lambda command and calculated lambda values in Figure 4 is to cross-validate the correlation between fuel enrichment and ammonia production. Although there is always a gap between the two lambda values, the changing trends in lambda showed consistency.

Similar to the 37km/h case, at 55km/h, the TWC temperature peaked at 670°C when the absolute engine load was increased to around 80%. Once the TWC temperature reached 670°C, the second COP was activated instantly. Compared with the "threshold" temperature at 37%, the "threshold" triggered at 55km/h was around 100°C

higher, plausibly due to the higher engine speed and quicker convection heat transfer. Due to the higher COP "threshold" temperature and the correspondingly larger amount of heat accumulated in the TWC monolith, the stabilization time of the second COP event almost doubled that of the first one. It can be seen in Figure 4 that the lambda of air-fuel mixtures was also enriched to 0.9 in the second COP event. This may be related to the manufacturer's default of engine calibration.

Some differences can be also noticed between the first and second COP events in Figure 3 and Figure 4. Although lambda was enriched to 0.9 in both cases once the COP strategy was activated, the ammonia concentrations measured at the tailpipe at 37km/h surged at a faster rate and to a higher level than those at 55km/h. This phenomenon seems slightly contradictory with the longer enrichment period in the second COP event. According to the concentrations of water vapor measured, a possible reason is the condensed water in the tailpipe. When liquid water presents, the reading of ammonia measurement becomes a dynamic balance among the formation, adsorption, and release of ammonia near the tailpipe exit, which significantly reduces the release rate of ammonia. In the second COP event, the relatively slower increase rate and peak concentration of ammonia could well support this theory.

The presence of liquid water not only changed the shape of the "rising edge" of ammonia emissions, but also impacted the decays after the COP enrichment stopped. As illustrated in Figure 3, at 37km/h, after fuel enrichment ended near 500s, ammonia could still be detected in the exhaust for quite a long time; it took roughly 350s to utterly clear the residual ammonia emissions (the time scale was in the same order of magnitude of wall storage attenuation ranging from 10 to 200s determined by Hoard [35]), which formed a tail-like shape of ammonia curvature. This behavior was a good example to show the influence of ammonia storage in sample lines. Since ammonia is a polar molecule gas, it can adsorb on and desorb from the inner surface of sample lines in addition to condensed water. This nature has been reported to possibly delay the response of measurement [35]. As shown in Figure 3 and Figure 4, it is plausible to hypothesize that part of the ammonia formed within the fuel enrichment durations might have first adsorbed on the inner surfaces of sample line, and then released and reentered the diluted exhaust via mass transfer when the ammonia concentration in the raw exhaust dropped. A similar phenomenon could be partially seen after the end of second COP event though the measurement was halted before the ammonia concentration went down to near zero.

The feature of ammonia solubility in water will pose a huge challenge for accurate quantification and sufficient repeatability if any forthcoming regulation is considering to include ammonia as a legislative pollutant for the purpose of abating secondary particulate matter precursors: Water-solubility will cause almost 100% sample loss in the CVS as the temperature inside is far lower than the boiling temperature of water. Besides, the intrinsically dynamic balance among formation, absorption, and release renders an integral of modal ammonia mass emission obtained using exhaust flow rate and raw concentration less scientifically viable. This problem doesn't exist for other regulated pollutants because of their very low water solubility.

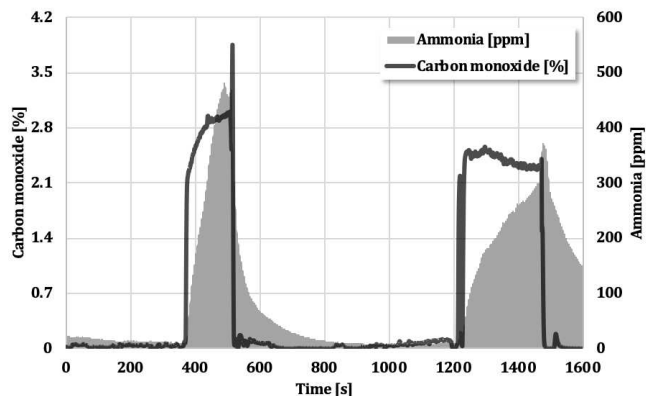## Correlation between ammonia and other pollutants during COP events

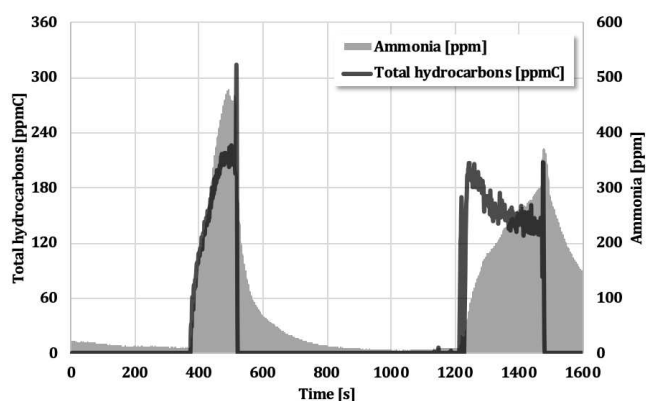Figure 5. Ammonia versus CO with the presence of COP

Figure 6. Ammonia versus THC with the presence of COP

Figure 3 and Figure 4 have confirmed the linkage between COP enrichment and extra ammonia emission from petrol vehicles. According to the formation mechanisms of ammonia on TWC which are given in reactions R1 to R11, CO and THC are both crucial precursors. Figure 5 and Figure 6 plot CO and THC with ammonia concentrations as a function of time to examine their correlations with ammonia during the two artificial COP events.

It can be observed in Figure 5 and Figure 6 that CO and THC showed similar responses to the fuel enrichment as the COP strategy was activated, but the CO concentrations were two orders of magnitude higher than those of THC, indicating that CO may play a more determinative role in the production of ammonia under fuel-rich conditions. In both COP events, ammonia concentrations peaked and began to dwindle when the "trailing edge" of CO and THC emerged. It is interesting to see in Figure 5 and Figure 6 that in the first COP event, both CO and THC concentrations increased with ammonia at the initial stage of fuel enrichment. This tendency aligned with the change in calculated lambda as plotted in Figure 4. However, during the second activation of COP strategy, CO and THC negatively correlated to ammonia concentration. Given that both the lambda command and calculated lambda values were relatively constant during the second COP event, the same mechanisms to form ammonia are probably occurring in both COP events. A plausible reason for the gradually descending CO and THC concentrations in the second COP event could be a consequence of reactive conversion

to ammonia, but this hypothesis needs to be validated with the testing of pre- and post-TWC data in future works.

To validate the intrinsic linkage between post-catalyst ammonia emission and other pollutants, the coefficients of correlation were calculated and listed in Table 4. As tabulated, the correlation between tailpipe ammonia and other pollutants was not so strong as visualized in the figures. A plausible reason that could be yielded from reactions R1 to R11 is that (not accounting for formed ammonia dissolved in condensed water) the production of ammonia on the TWC shall be proportional to the consumption of CO and THC, which are the differences between the inlet and outlet concentrations of TWC. It is thus difficult to accurately predict the of mass of ammonia production under fuel-rich conditions, but CO and THC can be good indicators of ammonia release as a hot TWC by-product. This theory agrees with the combustion incompleteness index proposed by Huang [19]. Besides, the effects of ammonia absorption and desorption in condensed water and on inner surfaces could to some extent bias the time alignment between ammonia and other pollutants, causing even poorer coefficients of correlation.

Table 4. Coefficients of correlation (power) between post-catalyst ammonia and other pollutants within COP events

	First COP	Second COP
CO	0.67	0.14
THC	0.57	0.17
CO_2	0.39	0.2
NOx	0.54	0.38
NO	0.76	0.01
NO_2	0.07	0
N_2O	0.57	0.03

Apart from carbonaceous pollutants CO and THC, the correlation between post-catalyst ammonia and the other three reactive nitrogen compounds, namely NO, NO_2, and N_2O measured by the same FTIR spectroscope, during the two COP events were also investigated. Their instantaneous emission concentrations were plotted as a function of time in Figure 7 to Figure 9, while the coefficients of correlation were given in Table 4.

It can be noticed in Figure 7 that the peaks of NO emission appeared when lambda rapidly switched from rich side to stoichiometry (around 520s and 1200s). It should be explained that the NO spike occurring around 670s belonged to the transition from 37km/h to 55km/h. Within the first COP event, the NO concentration maintained at a rather low level except the peak seen when fuel enrichment was cancelled. This may be due to a quite comprehensive conversion to nitrogen and ammonia. Whereas in the second COP window, the NO concentration became higher, which could be a result of elevated in-cylinder temperature as the absolute engine load increased. The changing tendency of NO emission within the second COP was also different from that in the first event but similar to those of CO and THC, where part of NO was consumed as a reactant to form ammonia.
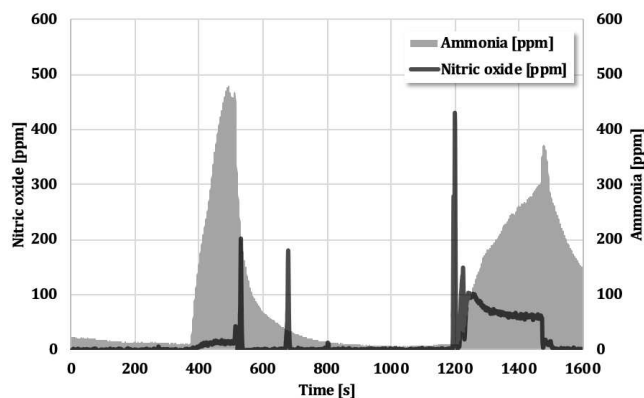
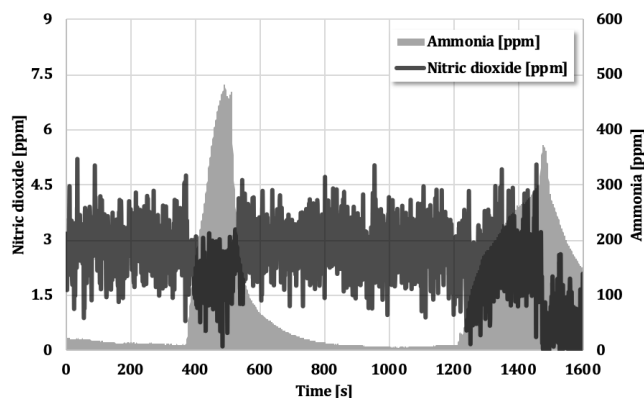Figure 7. Ammonia versus NO with the presence of COP
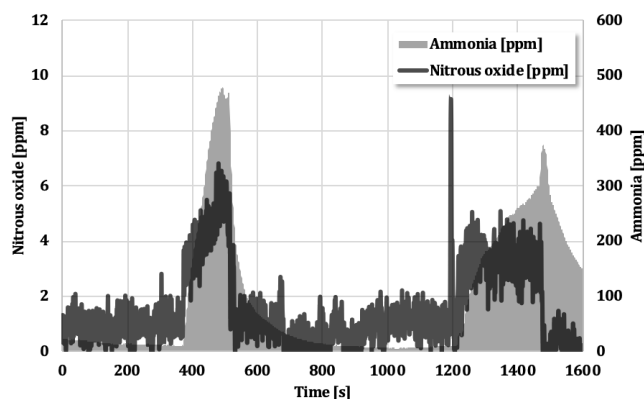

Figure 8. Ammonia versus NO_2 with the presence of COP

Figure 9. Ammonia versus N_2O with the presence of COP

In the whole testing process, the concentrations of NO_2 and N_2O were always below 10ppm as illustrated in Figure 8 and Figure 9. Due to the unstable nature of NO_2, lots of noise can be noticed in Figure 8. In general, NO_2 slightly declined as ammonia yielded with fuel enrichment in the first COP event, but this trend was not repeated when the second COP was activated because the change in NO_2 reading had been covered by measurement noise. In Figure 9, N_2O showed an analogous inclination with CO, THC, and NO emissions. Fuel enrichment within COP events also favored the production of N_2O though the increase in mass emission was almost negligible.

Summary

The ongoing discussion about complementing petrol ammonia emissions as a criteria pollutant in the next-phase emission regulations in the EU and China necessitate more comprehensive understanding of the mechanisms, sources, and control of post-catalyst ammonia from petrol vehicles.

Previous studies have shown that fuel enrichment and hot TWC catalyst are the governing driving factors of petrol ammonia formation. According to this theory, the catalyst overheating protection (COP) strategy employed by modern petrol vehicles could be a source of excessive ammonia emissions which hasn't received enough focus.

Using a self-programmed drive cycle, this research successively activated COP events at two constant speeds and, for the first time in literature, confirmed the intrinsic correlations among COP maneuvering, fuel enrichment, and the release of post-catalyst ammonia. Given that COP events could rarely happen in the process of certification tests but may possibly occur during routine driving, the real driving ammonia emissions from in-use vehicles could be somewhat underestimated or even overlooked by chassis-level tests, which necessitates the need for more on-road ammonia measurement.

Moreover, a non-negligible impact of ammonia absorption/desorption into condensed water occurred inside the exhaust sample line on the accurate quantification of ammonia was noticed in the tests, which could pose a major challenge for future legislation.

The coefficients of correlation between ammonia and other pollutants, including CO, THC, NO, NO_2, and N_2O, within the two COP events were also examined but no conclusion could be drawn as the coefficients were too low, but tailpipe CO and THC could still be used as indicators of ammonia formation with a hot TWC being the prerequisite. Given that only post-TWC pollutants were measured in this research, further testing of pre- and post-TWC concentrations will help elaborating more detailed pathways of ammonia formation and reliable correlations with other species within COP events.

References

1. Meng, W., Zhong, Q., Yun, X., Zhu, X., Huang, T., Shen, H., Chen, Y., Chen, H., Zhou, F., Liu, J., Wang, X., Zeng, E.Y., and Tao, S., "Improvement of a Global High-Resolution Ammonia Emission Inventory for Combustion and Industrial Sources with New Data from the Residential and Transportation Sectors," Environ Sci Technol 51(5):2821–2829, 2017, doi:10.1021/acs.est.6b03694.
2. Behera, S.N., Sharma, M., Aneja, V.P., and Balasubramanian, R., "Ammonia in the atmosphere: a review on emission sources, atmospheric chemistry and deposition on terrestrial bodies," Environ Sci Pollut R 20(11):8092–8131, 2013, doi:10.1007/s11356-013-2051-9.
3. Platt, S.M., Haddad, I.E., Zardini, A.A., Clairotte, M., Astorga, C., Wolf, R., Slowik, J.G., Temime-Roussel, B., Marchand, N., Ježek, I., Drinovec, L., Močnik, G., Möhler, O., Richter, R., Barmet, P., Bianchi, F., Baltensperger, U., and Prévôt, A.S.H., "Secondary organic aerosol formation from gasoline vehicle emissions in a new mobile environmental reaction chamber," Atmos Chem Phys 13(18):9141–9158, 2013, doi:10.5194/acp-13-9141-2013.

04/19/2022

4. Wang, X., Ge, Y., Gong, H., Yang, Z., Tan, J., Hao, L., and Su, S., "Ammonia emissions from China-6 compliant gasoline vehicles tested over the WLTC," Atmos Environ 199:136–142, 2019, doi:10.1016/j.atmosenv.2018.11.027.

5. Gu, B., Zhang, L., Dingenen, R.V., Vieno, M., Grinsven, H.J.V., Zhang, X., Zhang, S., Chen, Y., Wang, S., Ren, C., Rao, S., Holland, M., Winiwarter, W., Chen, D., Xu, J., and Sutton, M.A., "Abating ammonia is more cost-effective than nitrogen oxides for mitigating PM2.5 air pollution," Science 374(6568):758–762, 2021, doi:10.1126/science.abf8623.

6. Harkins, J.H. and Nicksic, S.W., "Ammonia in auto exhaust," Environ Sci Technol 1(9):751–752, 1967, doi:10.1021/es60009a002.

7. Smith, L.R. and Black, F.M., "Characterization of Exhaust Emissions from Passenger Cars Equipped with Three-Way Catalyst Control Systems," SAE Technical Paper, 1980, doi:10.4271/800822.

8. Carslaw, D.C. and Rhys-Tyler, G., "New insights from comprehensive on-road measurements of NOx, NO2 and NH3 from vehicle emission remote sensing in London, UK," Atmos Environ 81:339–347, 2013, doi:10.1016/j.atmosenv.2013.09.026.

9. Kean, A.J., Harley, R.A., Littlejohn, D., and Kendall, G.R., "On-Road Measurement of Ammonia and Other Motor Vehicle Exhaust Emissions," Environ Sci Technol 34(17):3535–3539, 2000, doi:10.1021/es991451q.

10. Heeb, N.V., Saxer, C.J., Forss, A.-M., and Brühlmann, S., "Trends of NO-, NO2-, and NH3-emissions from gasoline-fueled Euro-3- to Euro-4-passenger cars," Atmos Environ 42(10):2543–2554, 2008, doi:10.1016/j.atmosenv.2007.12.008.

11. Woodburn, J., Bielaczyc, P., and Szczotka, A., "Chassis Dynamometer Testing of Ammonia Emissions from Light-Duty SI Vehicles in the Context of Emissions of Reactive Nitrogen Compounds," SAE Technical Paper, 2013, doi:10.4271/2013-01-1346.

12. Borsari, V. and Assunção, J.V. de, "Ammonia emissions from a light-duty vehicle," Transp Res Part D Transp Environ 51:53–61, 2017, doi:10.1016/j.trd.2016.12.008.

13. Huai, T., Durbin, T.D., Miller, J.W., Pisano, J.T., Sauer, C.G., Rhee, S.H., and Norbeck, J.M., "Investigation of NH3 Emissions from New Technology Vehicles as a Function of Vehicle Operating Conditions," Environ Sci Technol 37(21):4841–4847, 2003, doi:10.1021/es030403+.

14. Link, M.F., Kim, J., Park, G., Lee, T., Park, T., Babar, Z.B., Sung, K., Kim, P., Kang, S., Kim, J.S., Choi, Y., Son, J., Lim, H.-J., and Farmer, D.K., "Elevated production of NH4NO3 from the photochemical processing of vehicle exhaust: Implications for air quality in the Seoul Metropolitan Region," Atmos Environ 156:95–101, 2017, doi:10.1016/j.atmosenv.2017.02.031.

15. Suarez-Bertoa, R. and Astorga, C., "Isocyanic acid and ammonia in vehicle emissions," Transp Res Part D Transp Environ 49:259–270, 2016, doi:10.1016/j.trd.2016.08.039.

16. Wang, C., Zheng, T., Lu, J., Wu, X., Hochstadt, H., and Zhao, Y., "Three-way catalytic reactions on Rh-based catalyst: Effect of Rh/ceria interfaces," Appl Catal Gen 544:30–39, 2017, doi:10.1016/j.apcata.2017.07.003.

17. Wang, C., Xia, W., and Zhao, Y., "New insight into hydroxyl-mediated NH3 formation on the Rh-CeO2 catalyst surface during catalytic reduction of NO by CO," Chinese J Catal 38(8):1399–1405, 2017, doi:10.1016/s1872-2067(17)62856-0.

18. Heeb, Norbert V., Christian J. Saxer, Anna-Maria Forss, and Stefan Brühlmann. "Correlation of Hydrogen, Ammonia and Nitrogen Monoxide (Nitric Oxide) Emissions of Gasoline-Fueled Euro-3 Passenger Cars at Transient Driving."

Atmospheric Environment 40, no. 20 (2006): 3750–63. https://doi.org/10.1016/j.atmosenv.2006.03.002.

19. Huang, C., Hu, Q., Lou, S., Tian, J., Wang, R., Xu, C., An, J., Ren, H., Ma, D., Quan, Y., Zhang, Y., and Li, L., "Ammonia Emission Measurements for Light-Duty Gasoline Vehicles in China and Implications for Emission Modeling," Environ Sci Technol 52(19):11223–11231, 2018, doi:10.1021/acs.est.8b03984.

20. Han, Y., Tan, J., Yang, J., Yang, Z., Ge, Y., Luo, J., and Hao, L., "Analysis of Factors Affecting Ammonia Emission from Gasoline Vehicles under WLTC Cycle," Research of Environmental Sciences 32(4):654-661.

21. Sun, K., Tao, L., Miller, D.J., Khan, M.A., and Zondlo, M.A., "On-Road Ammonia Emissions Characterized by Mobile, Open-Path Measurements," Environ Sci Technol 48(7):3943–3950, 2014, doi:10.1021/es4047704.

22. Nose, H., Inoue, T., Katagiri, S., Sakai, A., Kawasaki, T., and Okamura, M., "Fuel Enrichment Control System by Catalyst Temperature Estimation to Enable Frequent Stoichiometric Operation at High Engine Speed/Load Condition," SAE Technical Paper, 2013, doi:10.4271/2013-01-0341.

23. Heywood, John B. Internal combustion engine fundamentals. New York: McGraw-Hill. 1988.

24. Harvey, C.A., Garbe, R.J., Baines, T.M., Somers, J.H., Hellman, K.H., and Carey, P.M., "A Study of the Potential Impact of Some Unregulated Motor Vehicle Emissions," SAE Technical Paper, 1983, doi:10.4271/830987.

25. Durbin, Thomas D, Ryan D Wilson, Joseph M Norbeck, J.Wayne Miller, Tao Huai, and Sam H Rhee. "Estimates of the Emission Rates of Ammonia from Light-Duty Vehicles Using Standard Chassis Dynamometer Test Cycles." Atmospheric Environment 36, no. 9 (2002): 1475–82. https://doi.org/10.1016/s1352-2310(01)00583-0.

26. Livingston, Cody, Paul Rieger, and Arthur Winer. "Ammonia Emissions from a Representative In-Use Fleet of Light and Medium-Duty Vehicles in the California South Coast Air Basin." Atmospheric Environment 43, no. 21 (2009): 3326–33. https://doi.org/10.1016/j.atmosenv.2009.04.009.

27. Heeb, Norbert V., Anna-Maria Forss, Stefan Brühlmann, Roland Lüscher, Christian J. Saxer, and Paul Hug. "Three-Way Catalyst-Induced Formation of Ammonia—Velocity- and Acceleration-Dependent Emission Factors." Atmospheric Environment 40, no. 31 (2006): 5986–97. https://doi.org/10.1016/j.atmosenv.2005.12.035.

28. Bielaczyc, Piotr, Andrzej Szczotka, Antoni Swiatek, and Joseph Woodburn. "A Comparison of Ammonia Emission Factors from Light-Duty Vehicles Operating on Gasoline, Liquefied Petroleum Gas (LPG) and Compressed Natural Gas (CNG)." SAE International Journal of Fuels and Lubricants 5, no. 2 (2012): 751–59. https://doi.org/10.4271/2012-01-1095.

29. Bielaczyc, Piotr, Andrzej Szczotka, and Joseph Woodburn. "Regulated and Unregulated Exhaust Emissions from CNG Fueled Vehicles in Light of Euro 6 Regulations and the New WLTP/GTR 15 Test Procedure." SAE International Journal of Engines 8, no. 3 (2015): 1300–1312. https://doi.org/10.4271/2015-01-1061.

30. Suarez-Bertoa, R., A.A. Zardini, and C. Astorga. "Ammonia Exhaust Emissions from Spark Ignition Vehicles over the New European Driving Cycle." Atmospheric Environment 97 (2014): 43–53. https://doi.org/10.1016/j.atmosenv.2014.07.050.

31. Suarez-Bertoa, Ricardo, Alessandro A. Zardini, Velizara Lilova, Daniel Meyer, Shigeru Nakatani, Frank Hibel, Jens Ewers, Michael Clairotte, Leslie Hill, and Covadonga Astorga. "Intercomparison of Real-Time Tailpipe Ammonia Measurements from Vehicles Tested over the New World-

04/19/2022

Harmonized Light-Duty Vehicle Test Cycle (WLTC)." Environmental Science and Pollution Research 22, no. 10 (2015): 7450–60. https://doi.org/10.1007/s11356-015-4267-3.

32. Suarez-Bertoa, R., and C. Astorga. "Unregulated Emissions from Light-Duty Hybrid Electric Vehicles." Atmospheric Environment 136 (2016): 134–43. https://doi.org/10.1016/j.atmosenv.2016.04.021.

33. Suarez-Bertoa, Ricardo, Pablo Mendoza-Villafuerte, Francesco Riccobono, Michal Vojtisek, Martin Pechout, Adolfo Perujo, and Covadonga Astorga. "On-Road Measurement of NH3 Emissions from Gasoline and Diesel Passenger Cars during Real World Driving Conditions." Atmospheric Environment 166 (2017): 488–97. https://doi.org/10.1016/j.atmosenv.2017.07.056.

34. Li, H., Andrews, G.E., Savvidis, D., Daham, B., Ropkins, K., Bell, M., and Tate, J., "Comparisons of the Exhaust Emissions for Different Generations of SI Cars under Real World Urban Driving Conditions." SAE Technical Paper Series, 2008. https://doi.org/10.4271/2008-01-0754.

35. Hoard, J., Venkataramanan, N., Marshik, B., and Murphy, W., "NH3 Storage in Sample Lines," SAE Technical Paper, 2014, doi:10.4271/2014-01-1586.

Contact Information

Dr. Xin Wang, associate professor of National Laboratory of Automotive Performance & Emission Test, Beijing Institute of Technology, E-mail: xin.wang@bit.edu.cn

Dr. Daisy Thomas, lead automotive research engineer of 3DATX, E-mail: daisythomas@3datx.com

Definitions/Abbreviations

COP	catalyst overheat protection
CVS	constant volume sampling
ECU	engine control unit
FTIR	Fourier-transformation infrared analyzer
OBD	on-board diagnostic
SCR	selective catalytic reduction
TWC	three-way catalyst

04/19/2022